Hydraulic Jumps in Granular Material Flow

C. E. BRENNEN, K. SIECK* and J. PASLASKI*

California Institute of Technology, Pasadena, CA 91125 (U.S.A.)

(Received July 6, 1982)

SUMMARY

This paper investigates the formation of hydraulic jumps in the open channel flow of dry, cohesionless granular materials. The experimental observations include the identification of several types of jump and several types of downstream flow. The relation between the depth ratio across the jump and the Froude number is similar to that observed in the open channel flow of liquid. However, the ratio h_2/h_1 in the granular material case is larger by a factor of between 1.2 and 1.5 Analysis of this factor indicates that it is caused by a 10 to 20% reduction in the solid fraction below its critical value in the highly sheared supercritical flow upstream of the jump.

INTRODUCTION

The recent increase in research on the fundamental mechanics of the flow of dry granular materials has been stimulated, in part, by a desire to improve the core of knowledge needed for the efficient design of equipment used to transport and process large quantities of bulk material. Over the years, flows through hoppers under gravity have served as a useful rheological test for many postulated continuum models for dry granular material flow (for example, refs. 1, 2). More recently, there has been an effort toward laboratory examinations of other simple flows such as that in an annular shear cell [3]. As a contribution in this direction, we have been examining the flow of granular materials in an open channel inclined at various angles ϑ to the horizontal (see Fig. 1). The purpose of these investigations and this paper is twofold: first to provide useful engi-
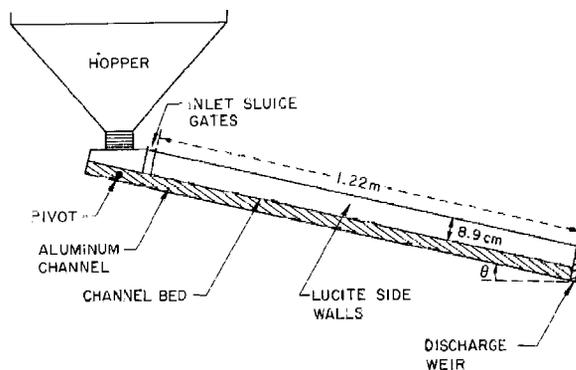
*Undergraduates.

Fig. 1. Schematic of channel used for granular material flows.

neering design data and second to permit fundamental tests of proposed constitutive laws of motion.

The present paper is concerned with one important aspect of the open channel flow of granular materials, namely that under certain conditions there exist hydraulic jumps analogous to those observed in the open channel flow of water. Hydraulic jumps have been reported previously by Savage [4], who also includes some analysis of the phenomenon as do Morrison and Richmond [5]. Here we shall present further detailed data on the relations between flows upstream and downstream of the jump and on the various flow structures which occur in the jump. Furthermore, we shall show that as well as the supercritical to subcritical transition inherent in any shock whether it be gas dynamic, hydraulic or of any other kind, a second structure can exist in granular media flow which permits a kind of reverse transition from subcritical flow to a 'landslide' type critical flow.

EXPERIMENTAL EQUIPMENT

The experiments were carried out in a small 122 cm long rectangular channel or chute

(Fig. 1) whose base was of polished aluminum (width b = 7.62 cm) and whose sides were of lucite (8.9 cm tall). Two lucite windows were inlaid in the base to observe the velocity of the material in contact with the base. The chute was pivoted at the upper end and could be clamped at a wide range of angles ϑ to the horizontal. The granular materials were fed to the top of the chute from a hopper and the flow regulated by an adjustable sluice gate at the upper end of the chute. An adjustable weir could also be fitted to the discharge end of the chute. Point probes at midspan were used to record the depth h of the flow to an accuracy of ±0.02 cm. In addition, profiles of the upper surface were obtained from photographs and from tracings through the lucite sidewalls. Mass flow rates m were obtained by timed collections of material discharging from the chute.

Three different granular materials were used: BT 4 glass beads, PO 170 glass beads and mustard seed with material properties as listed in Table 1. These materials were previously used in refs. 1, 2, 6, 7, 8 and 9 and 10 and the measurements are documented therein.

For the purposes of analysis of the results, the mass flow rates and depths were converted to dimensionless Froude numbers, and depth to particle size ratios $2h/d$; two Froude numbers Fr and Fr^* are used defined by

$$Fr = \frac{m}{\rho_P \nu_c bh(gh)^{1/2}}; \qquad Fr^* = \frac{Fr}{(\cos \vartheta)^{1/2}}$$

If the average solids fraction at a particular point was equal to ν_c, then Fr would represent the average material velocity divided by $(gh)^{1/2}$. However, in contrast to the open channel flow of a liquid, the average solids fraction or density at a particular location cannot be assumed to be known. Neither was it measured in the present study; indeed, it would be very valuable to devise experimental techniques for local solids fraction measurement in granular material flows.

In concert with the semantics of the open channel flow of liquid, flows with $Fr^* < 1$ or $Fr^* > 1$ will be referred to as subcritical or supercritical respectively.

CHUTE CHARACTERISTICS AND HYDRAULIC JUMP FORMATION

Without any obstruction in the channel, continuous steady state flows could only be generated when the angle of the chute was greater than a certain minimum value ϑ_{MIN}. This angle was about 24°, 19.5° and 24° for BT 4, PO 170 and mustard seed respectively, though it also appeared to depend on the upper sluice gate opening h_0.

It is important to note that in all cases ϑ_{MIN} is substantially less than the angle of repose because the friction angle between the material and the channel bed is considerably less than either the angle of repose or the internal friction angle. Between ϑ_{MIN} and another critical angle ϑ_{CRIT} (a few degrees larger than ϑ_{MIN}), flows in the unobstructed chute were subcritical and the value of h decreased with distance along the chute, such that the value of Fr^* at discharge was about unity. Under such conditions, the flow is choked at the chute exit. However, for $\vartheta > \vartheta_{CRIT}$, the flow in the chute is entirely supercritical and the flow is choked at or just upstream of the upper sluice gate. The specific value of ϑ_{CRIT} depends not only on the material but also on the gate opening h_0 and in particular on the length and breadth of the chute. For a detailed description of behavior of unobstructed chute flow, the reader is referred to ref. 6.

TABLE 1

Properties of granular materials used

	BT 4 glass beads	PO 170 glass beads	Mustard seed
Average particle diameter d (mm)	0.48	0.37	2.1
Angle of repose ϑ_R (degree)*	26.5	23.9	26.0
Internal friction angle φ (degree)**	25.8	24.6	
Wall friction angle** (degree) against			
(i) aluminum	13.2	17.7	
(ii) lucite	15.7	15.3	12.0
Particle specific gravity ρ_P	2.50	2.47	1.22
Critical solids fraction ν_c***	0.58	0.61	0.58

*Observation of maximum static slope.
**From shear cell tests.
***Minimum value from loose static packing tests.

For present purposes, it is sufficient to point out that even a minor obstruction placed in a subcritical flow almost always caused the flow to come to a halt. On the other hand, an obstruction placed in a supercritical flow can do one of two things. A small obstruction (say a point probe lowered into the flow) can simply cause a local acceleration of the flow in the neighborhood of the obstruction and thus generate a local depression in the free surface. On the other hand, a larger obstruction will cause the formation of a hydraulic jump which tends to propagate upstream. Depending on the position and size of the obstruction, the jump will either find an equilibrium position in the chute or propagate all the way to the upper sluice gate, at which time the entire flow will come to a halt. The jumps described in this report were all produced by obstructions placed at the chute exit and had reached a static equilibrium position; such flows were often maintained for lengthy periods of time with very little global change in the flow pattern or position of the jump. The position could be accurately controlled by minor changes in the extent of the obstruction at the exit. In this way, we ensured that the jump was not affected by local roughnesses in the chute bed, for example, at the location of the inlaid lucite windows. Furthermore, it was evident that the structure of the flow in the jump was *not* a function of its position in the chute, provided that the jump was more than about five downstream depths away from the obstruction. For shorter distances from the discharge obstruction, the local flow structures associated with the jump and with the flow past the obstruction began to interact.

HYDRAULIC JUMP TYPES

The jumps were characterized by the supercritical Froude number Fr_1 just upstream of the jump based on the measured mass flow rate and the depth h_1 of the flow (Fig. 2(a)). Two different patterns of flow within the jump were observed. At low values of Fr_1 the flow in the jump consisted of a smooth expansion (type X) as illustrated by Fig. 2(b). For larger Fr_1 the jump contains a recirculating eddy (type Y, Fig. 2(c)) necessarily accompanied by a stagnation line which was readily
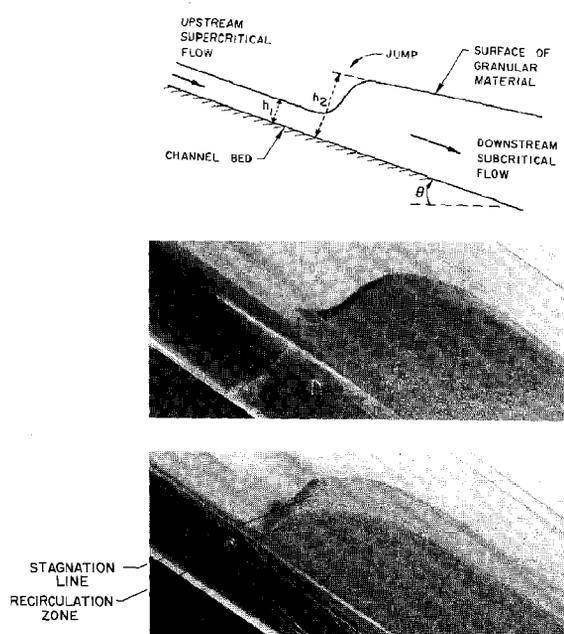

Fig. 2. (a) Schematic of a jump indicating the upstream and downstream depths, h_1 and h_2; (b) photograph of a typical jump without a recirculation zone (type X jump); (c) photograph of a typical jump with a recirculation zone and surface stagnation line (type Y jump).

observed from above. Unlike the highly unsteady mixing in a hydraulic jump in a liquid at high Reynolds numbers, this structure in the granular material jumps was steady, repeatable and readily distinguished. The substantially greater capacity for energy dissipation in the granular media case causes it to be more like jumps in a liquid at low Reynolds numbers.

The type of jump which occurred (X or Y) depended not only on the upstream Froude number Fr_1, but also on the channel inclination ϑ. The solid lines in Fig. 3 delineated the boundaries between the two types of jump for all three materials tested.

DOWNSTREAM FLOW

In contrast to the features of the jump itself, the subsequent development of the flow downstream of the jump depended to some extent on the nature and size of the obstruction. Though a sluice gate type of obstruction was also tried, the majority of the tests were performed with a flat plate weir at the end of the chute. In the analogous flow of liquid, the
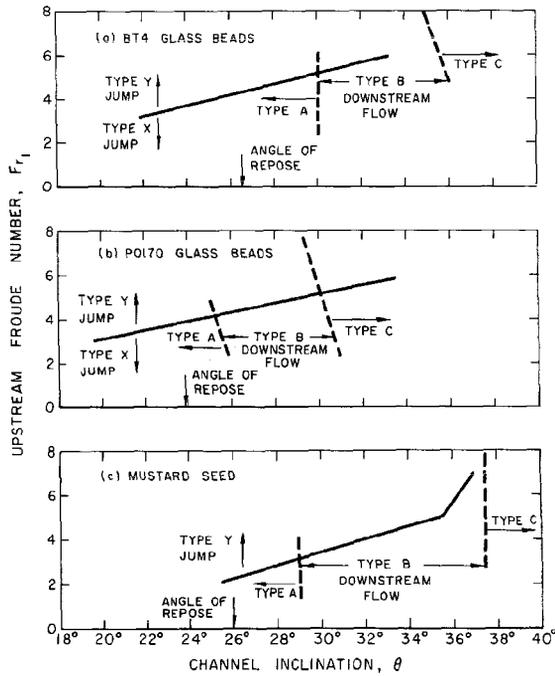
Fig. 3. Boundaries between the regimes of occurrence of jump types X and Y (solid lines) and of downstream flow types A, B and C; (a) BT 4 glass beads; (b) PO 170 glass beads; (c) mustard seed.

Fig. 4. Photographs of typical downstream flow types A (top), B (middle) and C (bottom).

height of the water surface above the weir h_w is determined by the condition that the Froude number Fr_w (based on h_w) is unity; the flow is choked at this point (ref. 2). In the present study, measurements of h_w for the three granular materials yielded values as follows:

	BT 4 glass beads	PO 170 glass beads	Mustard seed
Fr_w	0.933	1.041	0.744

indicating a similar behavior for the granular materials. The deviation in the case of mustard seed may be due to the substantially smaller value of h_w/d for that material.

Three basic types of flow (A, B. and C) occurred between the jump and the weir, depending on the channel inclination ϑ. For ϑ less than about (ϑ_R), the subcritical flow downstream of the jump was shearing over its entire depth and the only stagnant material present was a relatively small triangular region trapped behind the weir as shown in Fig. 4(a). This stagnant material was merely a local exit flow characteristic (an artifact of type of exit ob-
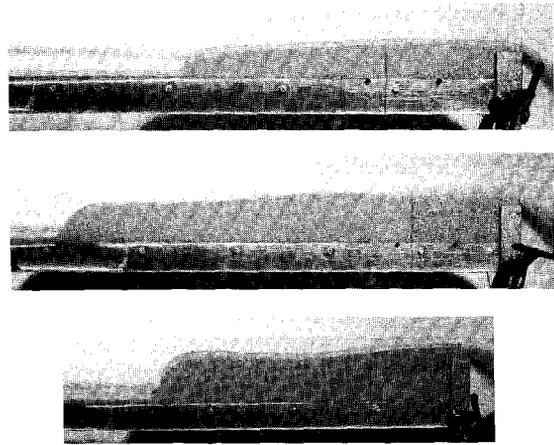
struction) since the sluice gate type obstruction exhibited a similar flow, except within a couple of depths of the exit. Flows downstream of the jump which exhibit shearing over their entire depth are designated as type A and their regime of occurrence is shown in Fig. 3, where the boundaries between different types of downstream flow are represented by dashed lines.

At channel inclinations greater than about (ϑ_R + 3), the flow downstream of the jump exhibited a more complex behavior (type B). To describe this, it is necessary to define a position along the chute where an imaginary plane drawn through the top of the weir at an inclination equal to the angle of repose intersects the bed of the chute; we refer to this as the critical repose point. For chute angles in a range between about (ϑ_R + 3) and (ϑ_R + 8), the jump positions itself well upstream of the critical repose point. Downstream of the jump, the entire depth of the flow is shearing as in type A. However, at about the critical repose point, the flow rides up over a stagnant wedge of material which is very much longer than the trapped stagnant material under the weir in type A. This transition is also characterized by a depression in the free surface as indicated in Fig. 4(b). Beyond this depression, both the inclination of the free surface and the boundary of the stagnant material were flat parallel planes inclined at the angle of repose. The Froude number of this overriding flow based on the depth of the shearing material was close to unity. (It ap-

pears that these are the conditions for a steady landslide.)

As the inclination of the chute is further increased, the jump moves downstream toward the critical repose point. The result is a hydraulic jump which is followed immediately by the formation of a base wedge as illustrated by Fig. 4(c) (type C downstream flow). Clearly this kind of jump is being affected by the nature of the obstruction downstream of the jump and by the associated overriding transition. It could be anticipated that such a structure would not occur in the case of a sluice gate obstruction. This proved to be the case. With a sluice gate, the flows were virtually all of type A.

The above discussion utilized crude approximate flow regime boundaries at $\vartheta = (\vartheta_R + 3)$ and $\vartheta = (\vartheta_R + 8)$. More accurate boundaries are shown as dashed lines in Fig. 3 for each of the three materials.

DEPTH RATIO ACROSS THE JUMP

A hydraulic jump is the physical manifestation between two conjugate states of an open channel flow. Therefore, it is simplest to neglect the small but finite length of the jump and to circumvent the effects of bed friction by extrapolation of the bed heights to a single location in the center of the jump. In the present study, the extrapolation of h_1 does not change that value. However, the effect of bed friction on the subcritical flow downstream of the jump causes a significant inclination of the free surface relative to the bed. Under these circumstances, the most appropriate downstream depth h_2 is obtained by extrapolating the downstream profile to the jump location as shown in Fig. 2.

It has been previously pointed out [4, 5] that in open channel flow of either liquid or granular material, the ratio h_2/h_1 is determined by the laws of mass conservation and momentum. In general, these lead to the following relation between h_2/h_1 and Fr_1^*:

$$2(Fr_1^*)^2 \left\{ \left(\frac{\beta_2}{\alpha_2^2}\right)\left(\frac{h_1}{h_2}\right) - \left(\frac{\beta_1}{\alpha_1^2}\right) \right\} = \delta_1 - \delta_2 \frac{h_2^2}{h_1^2} \quad (1)$$

where α, β, and δ are profile parameters to account for the variations in the velocity u and solids fraction ν, with elevation y above the chute bed and deviation of the pressure p from a purely hydrostatic variation with depth:

$$\alpha = \int_0^1 \frac{\nu}{\nu_c} \left(\frac{u}{\bar{u}}\right) d\left(\frac{y}{h}\right)$$

$$\beta = \int_0^1 \frac{\nu}{\nu_c} \left(\frac{u}{\bar{u}}\right)^2 d\left(\frac{y}{h}\right)$$

$$\delta = \int_0^1 \left\{ \frac{2p}{\rho_p \nu_c g h} \right\} d\left(\frac{y}{h}\right) \quad (2)$$

where $\bar{u}$ is the mean velocity and u, p and ν are functions of y in general. Equation (1) is essentially the same as that proposed by Morrison and Richmond [2] and later by Savage [4], except that they both propose specific forms for some of the profile parameter quantities. For example, the model used by Morrison and Richmond corresponds to values of $\delta_1 = (1 - \sin \varphi)/(1 + \sin \varphi)$, $\delta_2 = (1 + \sin \varphi)/(1 - \sin \varphi)$ and $\alpha = \beta = 1$ when the material is assumed cohesionless.

For the purposes of discussion, we also consider the following form of eqn. (1):

$$\frac{h_2}{h_1}\left(\frac{h_2}{h_1} + 1\right) = 2K(Fr_1^*)^2 \quad (3)$$

If, for example, $\alpha_1 = \alpha_2$, $\beta_1 = \beta_2$, $\delta_1 = \delta_2$, then eqn. (1) leads directly to eqn. (3) with $K = \beta/\alpha^2\delta$. The simple classic result for a hydraulic jump further assumes that all the profiles are such that α, β, and δ are unity and hence in this case $K = 1$.

The experimental values of h_2/h_1 are presented in Figs. 5(a), (b) and (c) as functions of Fr_1^* for each of the three materials tested. The data exhibit significant scatter due primarily to the difficulty in measuring the small upstream depth h_1. However, it is clearly seen that the granular material flows are qualitatively similar to conventional hydraulic jumps in that the relation between $h_2/h_1(h_2/h_1 + 1)$ and Fr_1^2 appears to be fairly linear. However, the slopes obtained (by least squares fits to the data of Fig. 4) are somewhat greater than 2 and correspond to the following values of the coefficient K.

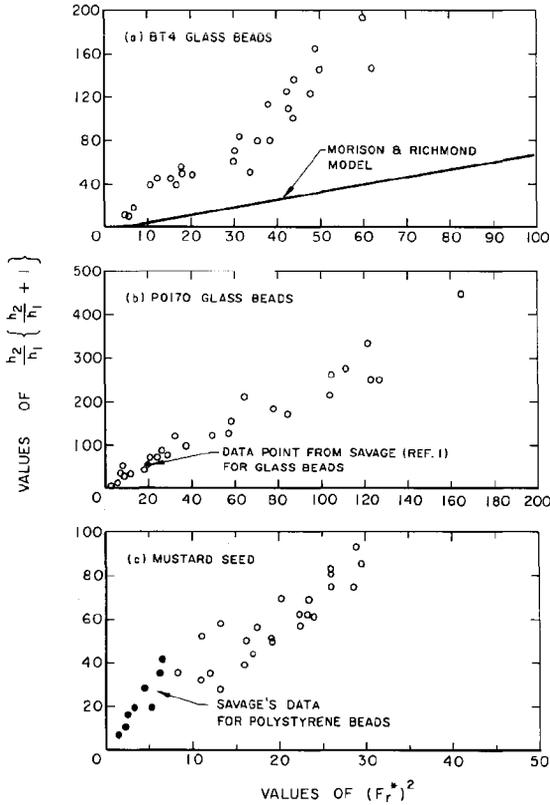|	BT 4 glass beads	PO 170 glass beads	Mustard seed
Effective coefficient K	1.33	1.22	1.46

Fig. 5. Data for the depth ratio across the jump plotted as $h_2/h_1(h_2/h_1 + 1)$ versus $(Fr_1^*)^2$; (a) BT 4 glass beads; (b) PO 170 glass beads; (c) mustard seed. Some data from Savage (ref. 1) for glass beads and polystyrene beads are also shown in the lower two graphs. Typical results for the Morrison and Richmond model (with $\varphi = 30°$) are shown in the top graph.

Within the level of the scatter, this coefficient seems to be unaffected by the type of jump (X or Y) or downstream flow (A, B or C). As in the case of the exit Froude numbers Fr_w, the mustard seed yields a value significantly different from that for the glass beads. In both cases, the deviations imply larger depths than expected on the basis of the glass bead results. This may be due to the larger size of particle.

Some data obtained by Savage [4] for relatively low Froude number flows of polystyrene particles and glass beads are also included in Figs. 5(b) and (c). These data are consistent with the present information.

Thus, the granular material jumps exhibit values of K significantly larger than unity. It is of interest to explore possible causes for this by considering non-unity values for the profile parameters. First we note from eqn. (1) that for values of h_2/h_1 greater than about 3 or 4, the parameters α_2, β_2 and δ_1 have rela-

tively little effect on the theoretical curves; the dominating parameters are α_1, β_1 and δ_2; then

$$K \approx \frac{\beta_1}{\alpha_1^2 \delta_2} \qquad (4)$$

Now consider the possible values of these parameters and their effect on the results. Consider first the δ_2 effect derived from a non-hydrostatic pressure profile in the shearing flow downstream of the jump. The model used by Morrison and Richmond [2] suggests a value of δ_2 greater than unity. Indeed, with a typical value of 30° for the internal friction angle, $\delta_2 = 3$. A more precise prediction of the Morrison and Richmond model using eqn. (1) with $\varphi = 30°$, $\delta_1 = 1/3$, $\delta_2 = 3$ and unit values for α_1, α_2, β_1 and β_2 is included in Fig. 5(a). It is clear that the effect on δ is a reduction rather than an increase in K and hence the model by itself appears inadequate to explain the observations. Therefore we turn to the effects of a solid fraction less than ν_c and to the influence of a non-uniform velocity profile. Consider first the latter in the absence of the former. Substantial velocity profiles could be observed in both the upstream and downstream flows, the velocity of the material in contact with the bed being about one-half of that at the surface. However, since $\bar{u}$ is defined as the mean velocity, the values of α will be equal to unity if $\nu = \nu_c$. Furthermore, the values of β caused by a linear profile with a base velocity one-half of the surface velocity is only 1.04. Such small deviations in β_1 seem insufficient to explain the results.

Finally we turn to the effect of a solids fraction ν less than ν_c and the subsequent effect on α_1, β_1 and δ_2. Note that a uniform value of ν/ν_c of about 0.85 (that is to say a 15% reduction in the solids fraction below its critical value) would lead to values of α, β and δ of 0.85 in the absence of other effects and hence to $K = 1.38$.

In summary, it would appear that the primary cause for values of K significantly larger than unity is a reduction in the solids fraction of the rapidly shearing flow upstream of the jump. Values of ν/ν_c in the range 0.8 to 0.9 would explain the observations. Such values are qualitatively consistent with the shear rate dependent dilations measured in shear flows by Savage and Sayed [3] and in channel flows by Ridgeway and Rupp [11].

CONCLUSIONS

Hydraulic jumps in the open channel flow of dry, cohesionless granular materials have been observed and categorized in this paper. Several types of jump as well as several types of the subsequent downstream flow are identified. In particular, the conditions under which the flow begins to override a stagnant understratum of material are identified. Such 'landslide' flows were observed to be governed by a Froude number of the order of unity.

The relation between the ratio of bed heights on either side of the jump and the Froude number is seen to be qualitatively similar to that for the open channel flow of liquid. However, the ratio h_2/h_1 is larger in the granular material jumps by a factor of 1.2 to 1.5. Analyses of the effects of solids fraction variation, non-uniform velocity profile and non-hydrostatic pressure gradient suggest that the primary cause is a 10 to 20% reduction in the solids fraction below its critical value in the highly sheared flow upstream of the jump.

ACKNOWLEDGMENTS

LIST OF SYMBOLS

b	width of the channel
d	particle diameter
Fr	Froude numbers defined in Experimental Equipment
g	acceleration due to gravity
h	depth of flow normal to channel bed
K	dimensionless coefficient
m	mass flow rate of granular material
p	normal stress on surface normal to channel bed
u	velocity of granular material parallel with channel bed
$\bar{u}$	volume average velocity. $\int_0^1 u \, d(y/h)$
y	co-ordinate measured normal to channel bed
α, β, δ	profile parameters of flow defined by eqn. (1)
φ	internal friction angle, degree
ϑ	inclination of channel to the horizontal, degree
ϑ_R	angle of repose, degree
ϑ_{MIN}	minimum channel inclination for flow, degree
ϑ_{CRIT}	a critical channel inclination (see Chute Characteristics)
ν	solids fraction
ν_c	critical solids fraction
ρ_P	particle specific gravity

Subscripts

0	conditions under inlet sluice gate
1	conditions upstream of jump
2	conditions downstream of jump
w	conditions at the discharge weir

REFERENCES

1 C. Brennen and J. C. Pearce, *J. Appl. Mech.*, Vol. 45, No. 1 (1978) 43 - 50.
2 T. V. Nguyen, C. Brennen and R. H. Sabersky, *J. Appl. Mech.*, Vo. 46 (1979) 529 - 535.
3 S. B. Savage and M. Sayed, *Experiments on dry cohesionless materials in an annular shear cell at high strain rates.* Presented at EUROMECH 133 — Statics and Dynamics of Granular Materials, Oxford Univ., (1980).
4 S. B. Savage, *J. Fluid Mech.*, Vol. 92, Part 1 (1979) 53 - 96.
5 H. L. Morrison and O. Richmond, *J. Appl. Mech.*, Vol. 43 (1976) 49 - 53.
6 C. E. Campbell, Ph.D. Thesis, California Institute of Technology (1982).
7 W. M. Sullivan. Ph.D. Thesis, California Institute of Technology (1982).
8 J. C. Pearce, Ph.D. Thesis, California Institute of Technology (1976).
9 T. V. Nguyen, Ph.D. Thesis, California Institute of Technology (1979).
10 J. K. Spelt, C. E. Brennen and R. H. Sabersky, *Int. J. Heat Mass Transfer*, submitted for publication (1982) (See also Report No. E200.3, Div. of Eng., Calif. Inst. of Tech.).
11 K. Ridgeway and R. Rupp, *Chem. and Proc. Eng.*, (May 1970) 82 - 85.